PCCP

Accepted Manuscript

This is an *Accepted Manuscript*, which has been through the Royal Society of Chemistry peer review process and has been accepted for publication.

Accepted Manuscripts are published online shortly after acceptance, before technical editing, formatting and proof reading. Using this free service, authors can make their results available to the community, in citable form, before we publish the edited article. We will replace this *Accepted Manuscript* with the edited and formatted *Advance Article* as soon as it is available.

You can find more information about *Accepted Manuscripts* in the Information for Authors.

Please note that technical editing may introduce minor changes to the text and/or graphics, which may alter content. The journal's standard Terms & Conditions and the Ethical guidelines still apply. In no event shall the Royal Society of Chemistry be held responsible for any errors or omissions in this *Accepted Manuscript* or any consequences arising from the use of any information it contains.

ROYAL SOCIETY OF CHEMISTRY

www.rsc.org/pccp

Journal Name RSCPublishing

COMMUNICATION

Photoelectrochemical hydrogen evolution of tapered silicon nanowires

Cite this: DOI: 10.1039/x0xx00000x

Received 00th January 2012,
Accepted 00th January 2012

DOI: 10.1039/x0xx00000x

www.rsc.org/

Xiaopeng Li,[ab] Yanjun Xiao,[c] Keya Zhou,[c] Junna Wang,[b] Stefan L. Schweizer,[b] Alexander Sprafke,[b] Jung-Ho Lee[*c] and Ralf B. Wehrspohn[*bd]

The origin of the photocurrent enhancement and the overpotential reduction in solar water splitting employing nanostructured silicon is still a matter of debate. A set of tapered Si nanowires (SiNWs) has been designed for clarifying the impact of nanostructured Si on the hydrogen evolution reaction (HER) while precisely tailoring several interference factors such as surface area, light absorption and a surface defect density. We find that defect passivation by KOH achieved by tapering is much more beneficial than the optical gain. Surfactant-mediated modification of SiNWs is capable of engineering the band structure. As a result, we suggest a guideline for nanostructured Si photoelectrodes optimized for the HER.

Broader context

Pursuing solar energy conversion devices with low cost and high efficiency has become a major task of scientists and engineers in our age. Photoelectrochemical (PEC) water splitting provides an alternative route to convert solar energy of intermittent nature into chemical fuels (i.e., H_2), which can be easily stored and transported. Nanostructured semiconductor photoelectrodes have shown the ability of remarkably improving the conversion efficiency, but many reports have simply ascribed the efficiency improvement to the enhancement of light absorption and surface area increase, without insightful considering various potential factors, such as band bending, surface recombination and surface chemistry. These factors at the nanoscale may greatly differ from the planar counterpart. Previous studies were unable to either exclude the interference factor, or to probe the exact changes in nanostructures, thus in-depth understandings have been compromised. We have investigated Si based nanostructures in this article. Utilizing a set of tapered Si nanowires (SiNWs), the effects of nanostructured Si on the PEC water splitting were clarified by precisely tailoring various interference factors. Combining our experimental and theoretical approaches, we find that the geometry of Si nanostructures plays a vital role in the efficiency improvement, and suggest practical guidelines for fabricating optimized Si nano-photoelectrodes.

Hydrogen is one of the most promising candidates to serve as the next-generation high-density energy storage media for fluctuating renewable energies.[1] Developing low-cost, stable and highly efficient photoelectrodes in photoelectrochemical (PEC) water splitting remains challenging. One prospective material to resolve this issue is silicon owing to its abundance, non-toxicity and a matured processing technology. However, high production cost of electronic-grade Si,[2] slow kinetics at the electrode[3] and a maximum quasi-Fermi-splitting of about 0.7 V[4] concomitantly hamper its commercial usefulness. Recent technological advancements[3,5-7] on nanostructured Si photoelectrodes were capable of orthogonalizing the directions between light capture and charge carrier collection along with superior light absorption. This approach utilized cheap, metallurgical-grade Si providing a short diffusion length of minority carriers.[8]

Nanostructured Si using a nanowire or nanoporous morphology has shown a photocurrent enhancement as well as the anodic on-set potential (V_{OS}) shift (≥400 mV) for the HER in sulfuric-acid electrolyte.[5,6] However, the absolute amount of photocurrent enhancement employing Si nanostructures varies in literatures in a large range. For instance, Oh *et al.* reported that the saturated photocurrent (J_{ph}) of nanoporous Si was ~1.2 times higher than that of planar structures.[5] The enhanced ratio was ~1.58 for nanoporous Si reported by U. Sim *et al.*,[6] and 1.2 for nanowires reported by Huwang *et al.*.[3] In addition, the origin of anodic V_{OS} shift has been controversially discussed in literatures in terms of surface area enhancement,[5] flat-band potential change,[3] or other possible factors.[8] A model and this design criteria for nanostructured Si photoelectrodes optimized for hydrogen production have not been reported yet.

Physical Chemistry Chemical Physics Accepted Manuscript

As the first step to approach this complex problem, we defined a model system which can be simply varied to verify the different possible contributions to the photocurrent enhancement and anodic V_{OS} shift. We utilized silicon nanowires (SiNWs) obtained by metal-assisted chemical etching (MaCE) as the basic structure and applied different one-step post-KOH etching procedures. Three major key issues can be addressed by the post-KOH etching. First, we could investigate how the surface defects originating from the fabrication process influence the PEC performance because the post-KOH etching decreased surface defects from the SiNWs proportionally to the etching time. Second, the surface roughness could also be precisely controlled while tuning the KOH etching time. Thus, the effect of surface roughness on PEC performance was separately revealed. Finally, the post-KOH etching tapers the SiNWs. This enabled us to study the shape effect on the HER. From the optical measurements along with our simulations, the tapered SiNWs were found to be an optically and electrically superior candidate for the hydrogen production. Based on our results, we suggested a guideline for designing Si photoelectrodes, which is rather different from previous theoretical approach reported in *Energy Environ. Sci., 2012, 5, 5203-5220.*[9]

I. Formation of tapered SiNWs and their optical properties

SiNWs were fabricated according to a typical two-step MaCE process.[8] Fig. 1(a) shows the SEM image of tapered SiNWs after post-KOH etching for 30 s. The detailed morphology evolution of SiNWs with the increasing post-KOH etching time was shown in the supporting information Fig. S1. From the cross-sectional images of Fig. S2 and TEM images of Fig. S3, some etching defects, i.e., tiny pores, can be observed at the tops of the original SiNWs. Note that the original SiNWs were agglomerated together. After KOH etching of 30 s, the SiNWs were separated from each other and their tips were sharpened. Such tapering processes were reported to originate from the higher etching rate in the <110> direction over the <100> direction at the top of the SiNWs.[10,11] SiNWs with small diameters (< 50 nm) can be easily removed during this process. Increasing further the KOH etching time leaded to a continuous dissolution of SiNWs along with rapid decrease in an areal density of SiNWs. Tapered SiNWs finally disappeared after 90 s etching, leaving behind a rugged Si surface. Fig. 1(b) shows the anodic current-voltage (J-V) curves of the different Si samples described above. Due to the formation of an anodic Si oxide film at the SiNW surfaces, the amount of anodic charges passing through the NW surfaces during the anodic passivation is proportional to the surface area.[3] Therefore, a possible measure of the surface roughness (γ) is:

$$\gamma = A_{Nano}/A_o = C_{Nano}/C_{Planar} \quad (1)$$

where A_{Nano} is a real surface area of the SiNW/electrolyte interface, A_o is the projected area, i.e., $\gamma = 1$ for a perfect planar Si. C_{Nano} and C_{Planar} are the amount of anodic charges upon anodic oxidation passing through the SiNWs and planar Si, respectively. The amount of anodic charges can be estimated by integrating the J-V curves. Fig. 1(b) shows the relationship between the γ values and KOH etching time. γ decreases almost linearly from 13.6 (as-prepared SiNWs) to 4.1 (90 s-etched SiNWs as a function of the etching time. The reflectance of SiNWs demonstrates a strong dependence on the post-KOH etching time. Despite a significant decrease of the areal density as well as a surface area of SiNWs upon post-KOH etching, the calculated averaged light absorption in the wavelength range of 300-1000 nm decreases only from 96.21% to 95.61% after 10 s etching and to 89.1% after 30 s etching (see Fig. 1(c)). In the near-UV region of 300-450 nm, tapered SiNWs (10-20 s etching) display a lower reflectance than the non-etched SiNWs (see Fig. 1(d)). The main reason is that the sharpening process of SiNWs leads to a gradual increase in volume fraction towards the NW bottoms causing a graded-refractive-index effect.[10] As a result, the optical impedance (refractive index) mismatch could be minimized at the interface between the tapered SiNWs and air. We have also simulated straight and tapered SiNWs at the same height and areal density (see SI for simulation detail) using the commercial software (COMSOL Multiphysics). Two kinds of nanostructures, i.e., periodic Si nanowires (SiNWs) and nanocones (SiNCs, same as tapered SiNWs) were employed for modeling. Moreover, Si nanofrustrums, i.e., nanocones with a flat head (SiNFs) was also chosen as the intermediate state between SiNWs and SiNCs. From Fig. 1(e), SiNCs showed much lower reflectance than SiNWs or SiNFs in wavelengths of 300-

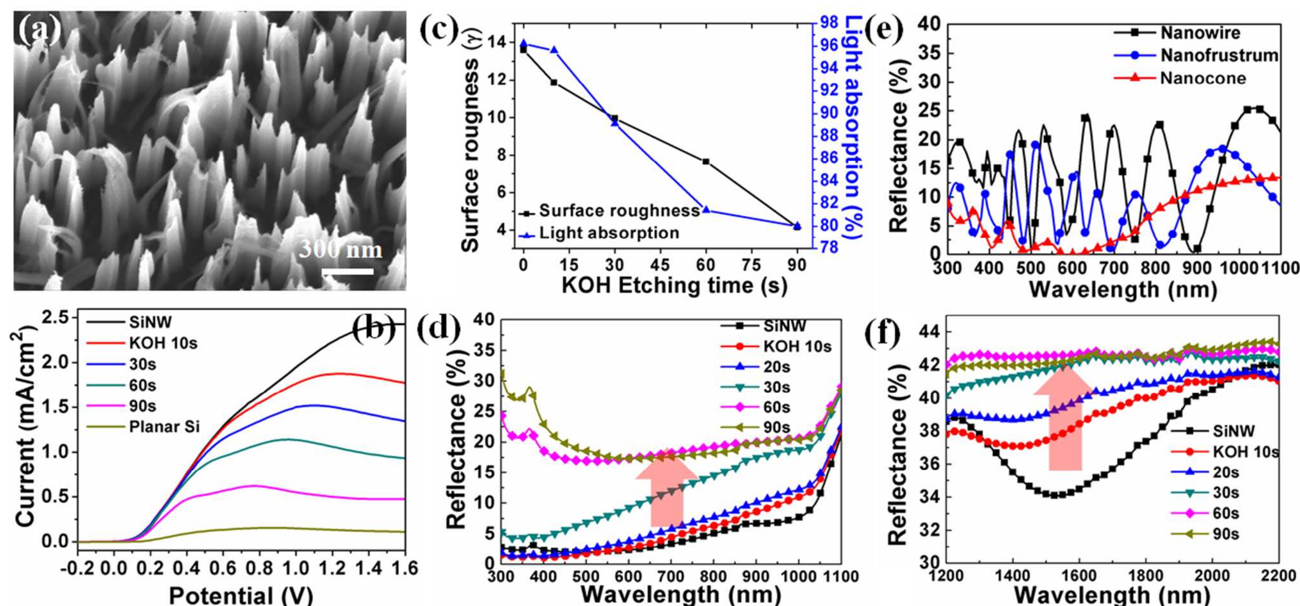

Figure 1. (a) Represented tilted-SEM view of tapered SiNWs with 30 s post-KOH etching time. (b) J-V curves for the different Si samples in a 0.5 M H_2SO_4 electrolyte. (c) Dependences of surface roughness and light absorption on the post-KOH etching time. (d) Total reflectance spectra of SiNWs with different post-KOH etching time in the wavelength ranges of 300–1100 nm. (e) Calculated reflectance spectra of silicon nanowires (NWs), nanofrustums (NFs) and nanocones (NCs). The detailed geometric parameters are given in the Supporting Information. (f) Total reflectance spectra of SiNWs with different post-KOH etching times in the wavelength ranges of 1200–2200 nm.

Physical Chemistry Chemical Physics Accepted Manuscript

1100 nm owing to the better matching in optical impedances between air and Si substrate.

The reflectance of SiNWs in the near-infrared (NIR) range (1200–2200 nm) shows the sub-bandgap light absorption in Fig. 1(f). Interestingly, there is a gradual increase of NIR light reflectance with the post-KOH etching time. Since the sub-bandgap light absorption is mainly due to the high-density of surface defect states,[12] the NIR light reflectance naturally increases according to a removal process of surface defects by KOH etching.

$$\frac{1}{\tau} = \frac{1}{\tau_{Bulk}} + \frac{S}{2d} \approx \frac{S}{2d} \qquad (2)$$

where τ_{Bulk} is the bulk lifetime of photogenerated minority carriers, which can be assumed to be infinite for ultrahigh pure Si; d is a sample thickness. Assuming the Shockley-Read-Hall recombination processes, S depends also upon the density of surface defect states[14]:

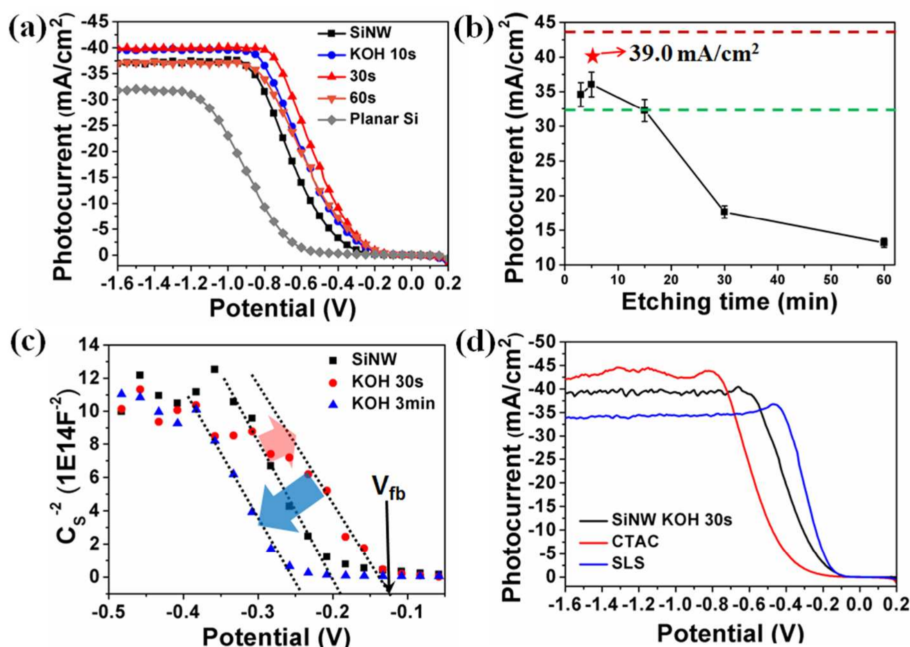

Figure 2. Photoelectrochemical (PEC) J-V curves of planar Si and SiNWs measured at 1-sun AM 1.5 illumination after different post-KOH etching times. (b) Saturated photocurrent values J_{ph} as a function of MaCE time. The red star denotes a J_{ph} value (39.0 mA/cm^2) of SiNWs after 30 s of KOH etching. The red dashed line denotes a theoretical maximum (43.6 mA/cm^2) of photocurrent. The green dashed line displays a saturated photocurrent value (32.2 mA/cm^2) of planar Si. (c) Mott-Schottky plots of SiNWs after different KOH etching times (measured at 1000 Hz): original SiNWs (black squares), KOH of 30 s (red circles), and KOH of 90 s (blue triangles). (d) PEC J-V curves of SiNWs after 30 s of KOH etching, which are measured with different surfactants: CTAC (red) and SLS (blue).

II. Effects of light absorption and surface defects on J_{ph}

Fig. 2(a) compares the PEC performances between planar Si and SiNWs after different KOH etching times. The original SiNWs (formed by MaCE for 5 min) shows an ~15% increase in J_{ph} as well as the anodic Vos shift of 400 mV compared to its planar counterpart, agreeing with previous reports.[3,5,6] Interestingly, after post KOH etching for 10 s, J_{ph} increases by more than 23 % than that of planar Si, along with an anodic V_{OS} shift of 500 mV. The J-V curve is shifted more positively by prolonging KOH etching to 30 s without changing a J_{ph} value. Further increasing the KOH etching time degrades the PEC performance.

Although the photocurrent enhancement mostly originated from the enhancement of light absorption as shown by the 60-s-treatment of KOH etching, J_{ph} of the tapered SiNWs has remained almost identically to that of the original SiNWs in spite of the absorption loss of ~20%. This feature implies that the electrons and holes generated from SiNWs likely recombine at the interface between electrolyte and SiNWs due to a high surface recombination velocity S, rather than effectively participate in the HER. Since S is related to the photogenerated minority carrier lifetime (τ) as follows,[13,14]

$$S = \nu_t \sigma N_{ss} \gamma \qquad (3)$$

where υ_t is the thermal velocity of the carriers, σ is the capture cross-section of the defects and N_{ss} is the microscopic density of surface defects per unit surface area. Combining the eq. (2) and (3), the ratio of surface defect density between SiNWs (N_{ssNano}) and planar Si ($N_{ssPlanar}$) is derived:

$$\frac{N_{ssNano}}{N_{ssPlanar}} = \frac{S_{Nano}}{\gamma S_{Planar}} = \frac{\tau_{Planar}}{\gamma \tau_{Nano}} \qquad (4)$$

Fig. S4 plots the carrier lifetime of planar Si (τ = 222.4 μs) and SiNWs (τ = 12.0 μs) chemically passivated (with hydrogen) using HF dip. The surface defect density enhancement per unit surface area in the SiNW sample was calculated to be $N_{SSnano}/N_{ssplanar}$ = 1.36 from eq. 4. The formation of these defects during MaCE is possibly due to the dissolution of Ag catalysts followed by renucleation of tiny Ag particles on the SiNW sidewalls during MaCE.[15] Thus, extending the MaCE time significantly degrades photocurrent due to the increased surface defect density (see Fig. 2(b)). Moreover, it is reasonable that the areal density of surface defects (i.e., tiny pores seen in Fig. S2 and S3) at the tops of NWs is higher because the NW tops are exposed to the etchant for longest time in comparison to

Physical Chemistry Chemical Physics Accepted Manuscript

other parts of the SiNWs. Conversely, taking advantage of anisotropic properties of KOH etching, defects can be removed in a controlled manner to improve the photocurrent being in line with the change in the NIR light reflectance of the samples.

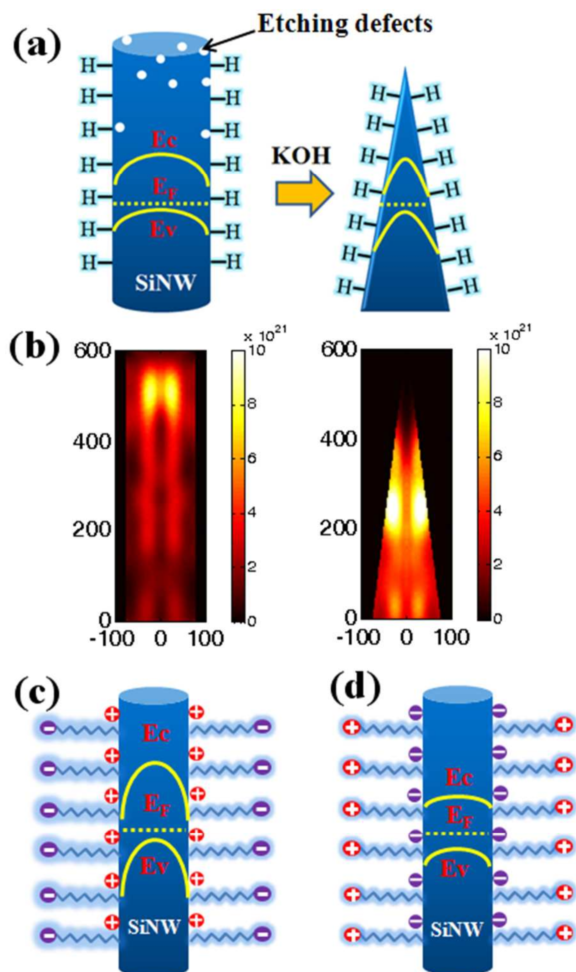

Figure 3. (a) Schematic of the SiNWs tapering process by the post-KOH etching. H represents the hydrogen termination. E_C, E_F and E_V are the conduction band, Fermi level and valence band of Si, which are marked as yellow line. (b) Calculated electron generation rates for straight SiNWs and tapered SiNWs under one AM1.5 solar irradiation. Schematics of (c) anionic and (d) cationic surfactants on the band bending in SiNW. Purple and red circles represents negative and positive charges respectively.

III. The origin of the anodic shift of V_{OS}

Another interesting finding of our study is that even though the surface area is reduced, tapered SiNWs show a larger anodic shift of V_{OS} (Fig. 2(a)). This finding might be a key in understanding of the origin of the V_{OS} shift. We suggest that the V_{OS} shift can be directly related to the increased “surface charge modulation (SCM)” effect. It is well documented that different surface terminates (e.g., $-CH_3$, -Cl, -H) or absorbates (e.g., H_2O, ionic surfactants) induce charge accumulation on the semiconductor surface thereby decreasing or increasing the band bending in the space charge region.[16-19] In comparison with the planar counterpart, such effect in silicon nanostructures would be much more remarkable in changing the band bending due to their high surface-to-volume ratio. As shown in the Fig. 3(a), the surface terminates H creates positive charge accumulation at the Si surface and attract electrons from the Si core to the surface leading to the strengthened downward band bending.[20] Due to such change of the electrostatic properties of the surface, the separation of photon generated charge carriers is improved resulting in the enhancement of photocurrent and photovoltage. Once the surface-to-volume ratio of SiNWs is increased via adjusting the post-KOH etching time, the V_{OS} shifts more anodically. The flat band potential shift with the increasing of post-KOH etching time shown in Fig. 2 (c) also confirmed the enhanced downward band bending in line with the previous report.[19]

For the further verification of our concept of the SCM effect, two kinds of chemical surfactants including anionic surfactant sodium lauryl sulfate (SLS) and cationic surfactant cetyl trimethylammonium chloride (CTAC) were added to the electrolyte. Fig. 2(d) shows their influence on the PEC performance. SLS shifted the J-V curve even more anodically, and CTAC shifts in the opposite cathodic direction. Fig. 3(c, d) shows the band bending change induced by surfactants. For SLS, its alkyl tail would adsorb at the NW surface, and the negative charged head group would point to the solution side. According to a previous report,[19] positive surface dipoles form at Si surface under such circumstances. These positive dipoles attract electrons to SiNW surface causing enhanced downward band bending. In contrast, for CTAC, surface band bending in SiNWs is weakened due to the formation of negative surface diploes. The addition of surfactants also influenced J_{ph}, CTAC improved the photocurrent to J_{ph} = 42.5 mA/cm^2, approaching the theoretical limit. On the contrary, SLS reduced the photocurrent to J_{ph} = 32.5 mA/cm^2. This phenomenon suggests that chemical surfactants not only own the ability to change the band bending, but also have the possibility to modulate the electronic properties of Si nanostructures by reducing or increasing the surface recombination.

IV. Design considerations for solar water splitting

To understand the superior performance of tapered SiNWs, we simulated the electron generation rates throughout the structure and demonstrated their distribution in the cross-section through the center of SiNWs and tapered ones (simulation details seen SI). As shown in Fig. 3(b), the electron generation rate G_{el} in tapered SiNWs (in the simulation approximated as the SiNCs) is on average ~40% higher than that in original SiNWs. More interestingly, we find that the strongest electron generation rate region ($G_{el} = 8\times10^{21}$ electrons per cm^3) is located at the top of SiNWs, where many etching defects existed and acted as recombination centers. In contrast for tapered ones, the strongest electron generation rate is located at the upper middle region ($G_{el} = 1\times10^{22}$ electrons per cm^3), well matching the strong band bending shown in Fig. 3(a). As a result, the photocurrent of tapered SiNWs is much higher than that of SiNWs, which is in accordance with our experimental data. Once the surface was properly passivated, the photocurrent can easily almost achieve close to the theoretical limit J_{ph} = 43.6 mA/cm^2. In the case of designing highly efficient nanostructured Si based water splitting devices, the region of the highest electron generation rate should correlate with the region of enhanced band bending while avoiding defect-rich regions in the nanostructures. For commonly used Si nanostructures by MaCE or other technologies, we strongly suggested removing the top part of nanostructures where there are lots of surface damages and etching defects.

Conclusions

Physical Chemistry Chemical Physics Accepted Manuscript

This journal is © The Royal Society of Chemistry 2012

In summary, we have fabricated a model system to address the origin of the enhanced photocurrent and the origin of the anodic shift if the Vos in nanostructured Si electrodes during solar hydrogen evolution. We find that instead of optimizing the light absorption in nanostructured Si, controlling the surface defect density is crucial for achieving a high photocurrent. Post KOH etching treatments can effectively remove the defects without sacrificing much light absorption. Our model system of tapered SiNWs has provided evidence that the anodic shift of V_{OS} is due to the SCM effect. Note that Si-H remains stable only for hours during the HER, therefore further improving the surface passivation chemistry is crucial for long term stability; meanwhile the electronic properties of nanostructured Si such as surface band bending and surface recombination velocity can also be effectively modulated. Combining theoretical simulations and the experimental approaches, we verified that tapered SiNWs or nanocones are an excellent candidate for the photoelectrochemical HER. With a careful surface passivation, the efficiency of tapered SiNWs can achieve close to the theoretical limit of silicon.

Acknowledgements

X. Li is grateful for the financial support from International Max-Planck Research School (IMPRS) and acknowledge the financial support from the National Natural Science Foundation of China (No. 21403280). Y. Xiao is grateful for the support from the China Scholarship Council (CSC). We thank Prof. Michael Bron for his kind help in electrochemical measurements.

Notes and references

[a] Max-Planck Institute of Microstructure Physics, Weinberg 2, Halle D-06120, Germany.
[b] Institute of Physics, Martin-Luther-Universität Halle-Wittenberg, Germany.
[c] Department of Chemical Engineering, Hanyang University, Ansan, Kyounggi 426-791, Korea.
[d] Fraunhofer Institute for Mechanics of Materials IWM Halle D-06120, Germany .

Electronic Supplementary Information (ESI) available: [details of any supplementary information available should be included here]. See DOI: 10.1039/b000000x/

1. J. A. Turner, *Science*, 2004, **305**, 972.
2. A. Luque and S. Hegedus, Handbook of Photovoltaic Science and Engineering. 2nd Ed. John Wiley and Sons, 2011; Chap. 5.
3. I. Oh, J. Kye and S. Hwang, *Nano Lett.*, 2012, **12**, 298.
4. L. Vayssieres, On solar hydrogen and nanotechnology. 1st Ed. John Wiley and Sons, 2010.
5. J. Oh, T. G. Deutsch, H.-C. Yuan and H. M. Branz, *Energy Environ. Sci.*, 2011, **4**, 1690.
6. U. Sim, H.-Y. Jeong, T.-Y. Yang and K. T. Nam, *J. Mater. Chem. A*, 2013, **1**, 54140
7. J.-Y. Jung, M. J. Choi, K. Zhou, X. Li, S.-W. Jee, H.-D. Um, M.-J. Park, K.-T. Park, J. H. Bang, J.-H. Lee, *J. Mater. Chem. A*, 2014, **2**, 833.
8. X. Li, Y. Xiao, J. H. Bang, D. Lausch, S. Meyer, P.-T. Miclea, J.-Y. Jung, S. L. Schweizer, J.-H. Lee, R. B. Wehrspohn, *Adv. Mater.*, 2013, **25**, 3187.
9. J. M. Foley, M. J. Price, J. I. Feldblyum and S. Maldonado, *Energy Environ. Sci.*, 2012, **5**, 5203.
10. J.-Y. Jung, Z. Guo, S.-W. Jee, H.-D. Um, K.-T. Park and J.-H. Lee, *Opt. Exp.*, 2010, **18**, A286.
11. X. Li, H.-S. Seo, H.-D. Um, S.-W. Jee, Y. W. Cho, B. Yoo and J.-H. Lee, *Electrochim. Acta*, 2009, **54**, 6978.
12. L. Tsakalakos, J. Balch, J. Fronheiser, M.-Y. Shih, S. F. LeBoeuf, M. Pietrzykowski, P. J. Codella, B. A. Korevaar, O. Sulima, J. Rand, A. Davuluru and U. Rapol. *J. Nanophotonics*, 2007, **1**, 013552.
13. N. S. Lewis, *Inorgan. Chem*. 2005, **44**, 6900.
14. K. Hagedorn, C. Forgacs, S. Collins and S. Maldonado, *J. Phys. Chem. C*, 2010, **114**, 12010.
15. X. Li, Y. Xiao, C. Yan, K. Zhou, P.-T. Miclea, S. Meyer, S. L. Schweizer, A. Sprafke, J.-H. Lee and R. B. Wehrspohn, *Electrochimica Acta*, 2014, **138**, 476.
16. J.-N. Chazalviel, *J. Electroanal. Chem.*, 1987, **233**, 37-48.
17. N. Alderman, L. Danos, M. C. Grossel and T. Markvart, RSC Advances, 2012, 2, 7669-7672.
18. D. C. Gleason-Rohrer, B. S. Brunschwig and N. S. Lewis, *J. Phys. Chem. C*, 2013, **117**, 18031-18042.
19. F. Camacho-Alanis, H. Castaneda, G. Zangari and N. S. Swami, Langmuir, 2011, 27, 11273.
20. C.-S. Guo, L.-B. Luo, G.-D. Yuan, X.-B. Yang, R.-Q. Zhang, W.-J. Zhang and S.-T. Lee, *Angew. Chem. Int. Ed.,* 2009, **121**, 10080.

Physical Chemistry Chemical Physics Accepted Manuscript